MECHANICS

Original article
DOI: https://doi.org/10.18721/JPM.15315

FUNCTIONALLY GRADED WEDGE WEAKENED BY A SEMI-INFINITE CRACK

V. V. Tikhomirov✉

Peter the Great St. Petersburg Polytechnic University, St. Petersburg, Russia

✉ victikh@mail.ru

Abstract. In the paper, the problem of a semi-infinite antiplane interface crack located between two functionally graded wedge-shaped regions has been considered. The shear modules of the materials' regions are quadratic functions of the polar angle. This kind of functional inhomogeneity made it possible to express all the components of the elastic field through a single harmonic function. Using the Mellin integral transform, the problem was reduced to the Wiener – Hopf scalar equation, for which an exact solution was obtained. The influence of gradients of elastic properties of materials on the stress intensity coefficient at the crack tip and the singularity value at the angular point of the structure was studied.

Keywords: functionally graded wedge, antiplane interface crack, stress singularity

Citation: Tikhomirov V. V., Functionally graded wedge weakened by a semi-infinite crack, St. Petersburg State Polytechnical University Journal. Physics and Mathematics. 15 (3) (2022) 201–213. DOI: https://doi.org/10.18721/JPM.15315

Научная статья
УДК 539.3
DOI: https://doi.org/10.18721/JPM.15315

ФУНКЦИОНАЛЬНО-ГРАДИЕНТНЫЙ КЛИН, ОСЛАБЛЕННЫЙ ПОЛУБЕСКОНЕЧНОЙ ТРЕЩИНОЙ

В. В. Тихомиров✉

Санкт-Петербургский политехнический университет Петра Великого,

Санкт-Петербург, Россия

✉ victikh@mail.ru

Аннотация. Рассматривается задача о полубесконечной антиплоской интерфейсной трещине, находящейся между двумя функционально-градиентными клиновидными областями. Модули сдвига материалов областей являются квадратичными функциями полярного угла. Такой вид функциональной неоднородности позволяет выразить все компоненты упругого поля через одну гармоническую функцию. С помощью интегрального преобразования Меллина проблема сведена к скалярному уравнению Винера – Хопфа, для которого получено точное решение. Изучено влияние градиентов упругих свойств материалов на коэффициент интенсивности напряжений в вершине трещины и показатель сингулярности в угловой точке структуры.

Ключевые слова: функционально-градиентный клин, антиплоская интерфейсная трещина, сингулярность напряжений

Ссылка для цитирования: Тихомиров В. В. Функционально-градиентный клин, ослабленный полубесконечной трещиной // Научно-технические ведомости СПбГПУ. Физико-математические науки. 2022. Т. 15. № 3. С. 201–213. DOI: https://doi.org/10.18721/JPM.15315

Introduction

Functionally graded materials (FGM) are composites whose mechanical and physical properties reflect the characteristics of their spatially variable microstructure [1, 2]. The concept of FGM was first introduced in the 1980s in Japan, finding wide application in the aerospace and nuclear industries, electronics, optoelectronics, construction and other fields as materials for energy conversion and as biomaterials [3]. Simulations consider FGM as heterogeneous materials, assuming the variation in their properties to be continuous, while their microstructure is not taken into account in this case.

Analysis of stress field singularities in such materials is one of the fundamental problems in linear fracture mechanics [4]. Due to the gradient of elastic properties, the classical nature of stress singularity (square-root in the case of cracks and simple power-law in the case of sharp notches) can be modified in the FGM [5, 6].

Numerous studies have considered fracture in FGM in the plane and antiplane formulations. Confining ourselves to antiplane problems, we should note that one of the first studies in this direction [7] established that the jump in the derivative of the shear modulus (preserving its continuity) does not affect the singularity exponent at the crack tip.

Singular fields in layered structures with functionally graded elements which have defects such as cracks oriented along or perpendicular to the gradient of the shear modulus were considered in [8–11]. The stress-strain state of wedge-shaped regions with gradient properties, including multi-material wedges and sharp notches were described in [5, 6, 12–14].

The dependence of the FGM shear modulus on the coordinates is selected in analytical models from a class of functions for which the equilibrium equations have analytical solutions. Linear or exponential dependences are typically used for the shear modulus. If the elastic module varies arbitrarily, the piecewise linear and piecewise exponential models can be applied [15, 16]. A quadratic dependence of the shear modulus on the polar angle was proposed in an earlier study [13] for gradient material, allowing to express all the components of the elastic field in terms of a single harmonic function under the conditions of an antiplane problem. This approach was used for singularity analysis in the apex of a multi-material wedge [14].

Based on the results obtained in [13], we consider the stress state of a composite wedge with gradient properties varying quadratically in the transverse direction, weakened by a semi-infinite antiplane crack. The effect from the increase and decrease in the stress intensity factor (SIF) at the tip of the crack has been analyzed, as well as the variations in the singularity exponent in the corner of the wedge due to gradient elastic properties of materials, compared to a homogeneous structure.

Problem statement

Consider a semi-infinite mode III interface crack located between two wedge-shaped regions Ω_1 and Ω_2 with the angles α_1 and α_2 (Fig. 1):

$$\Omega_1 = \{(r,\theta): 0 < r < \infty, 0 < \theta < \alpha_1\},\ \Omega_2 = \{(r,\theta): 0 < r < \infty, -\alpha_2 < \theta < 0\},$$

where r, θ are the polar coordinates.

It is assumed that the materials in these regions are functionally graded, and their shear moduli μ_1 and μ_2 are functions of the polar angle. In this case, the functional dependences $\mu_k(\theta)$ ($k = 1, 2$) are such that the elastic moduli are the same on the ray $\theta = 0$, equal to μ_0, taking the values μ_* at the boundaries $\theta = \alpha_1$ and $\theta = -\alpha_2$.

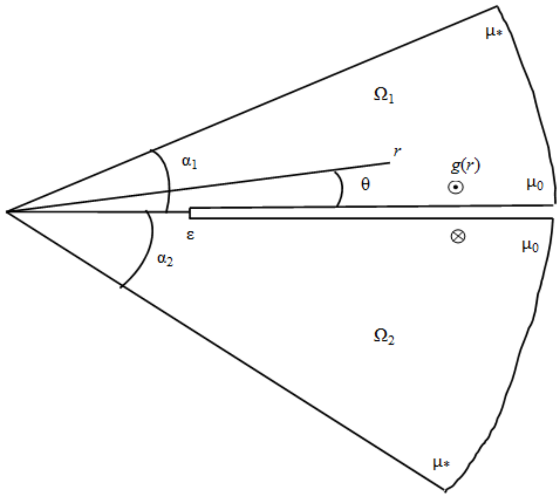

Fig. 1. Functionally graded wedge with semi-infinite interface crack under longitudinal shear: μ_1, μ_2 are the shear moduli at the boundaries of the regions Ω_1 and Ω_2 with graded materials; α_1, α_2, θ, r, ε are the geometric parameters; $g(r)$ is a self-balanced load applied to the edges of the crack

We assume that the tip of crack is located at a distance ε from the apex of a composite wedge. A self-balanced load $g(r)$ is applied to the edges of crack. The contact of materials outside the crack is assumed to be perfect.

The equilibrium equations take the following form in the regions Ω_k with shear moduli varying in the transverse direction

$$\frac{\partial^2 w_k}{\partial r^2}+\frac{1}{r^2}\frac{\partial^2 w_k}{\partial\theta^2}+\frac{1}{r}\frac{\partial w_k}{\partial r}+\frac{1}{\mu_k(\theta)r^2}\frac{d\mu_k}{d\theta}\frac{\partial w_k}{\partial\theta}=0, \tag{1}$$

and the stresses are expressed in terms of displacements $\tilde{w}_k$ by the following formulas:

$$\tau_{\theta zk}=\frac{\mu_k}{r}\frac{\partial w_k}{\partial\theta},\ \tau_{rzk}=\mu_k\frac{\partial w_k}{\partial r}\ \ (k=1,2). \tag{2}$$

Consider a quadratic functional dependence of the shear modulus in FGM on the polar angle, proposed and tested in [12]:

$$\mu_k(\theta)=(a_k\theta+b_k)^2, \tag{3}$$

where the coefficients in this case take the form

$$a_k=(\sqrt{\mu_*}-\sqrt{\mu_0})/\alpha_k,\ b_1=-b_2=\sqrt{\mu_0}.$$

Therefore, the shear modulus of the composite is continuous at the interface $\theta = 0$, and its derivative with respect to the angle θ has a discontinuity.

Searching for displacements in the regions Ω_k in the form

$$w_k(r,\theta)=\frac{1}{a_k\theta+b_k}\tilde{w}_k(r,\theta) \tag{4}$$

from Eqs. (1), we obtain that the functions $\tilde{w}_k(r,\theta)$ are harmonic:

$$\frac{\partial^2 \tilde{w}_k}{\partial r^2}+\frac{1}{r^2}\frac{\partial^2 \tilde{w}_k}{\partial \theta^2}+\frac{1}{r}\frac{\partial \tilde{w}_k}{\partial r}=0. \quad (5)$$

Using Eqs. (2), we arrive at the following representations for the stresses:

$$\tau_{\theta zk}=-\frac{a_k}{r}\tilde{w}_k(r,\theta)+\frac{a_k\theta+b_k}{\mathrm{r}}\frac{\partial \tilde{w}_k}{\partial \theta}, \quad (6)$$

$$\tau_{rzk}=(a_k\theta+b_k)\frac{\partial \tilde{w}_k}{\partial r}.$$

Solutions of Eqs. (1) at the interface θ = 0 must satisfy mixed conditions

$$\tau_{\theta z1}(r,+0)=\tau_{\theta z2}(r,-0),\ w_1(r,+0)=w_2(r,-0)\ (0\le r\le 1), \quad (7)$$

$$\tilde{\tau}_{\theta z1}(r,+0)=\tilde{\tau}_{\theta z2}(r,-0)=g(r)\ (1\le r<\infty),$$

as well as boundary conditions at the edges of the wedge

$$\tau_{\theta z1}(r,\alpha_1)=0,\ \tau_{\theta z1}(r,-\alpha_2)=0\ (0\le r<\infty). \quad (8)$$

Reducing the problem to the Wiener–Hopf equation and its solution

We search for the solution of problem (1)–(8) in the regions Ω_k in the form of Mellin integrals:

$$w_k(r,\theta)=\frac{1}{2\pi i}\int_L W_k(p,\theta)r^{-p}dp\ (k=1,2), \quad (9)$$

$$W_k(p,\theta)=[A_k(p)\sin p\theta+B_k(p)\cos p\theta]/(a_k\theta+b_k).$$

According to Eqs. (6), stresses are defined by expressions

$$\tau_{\theta zjk}(r,\theta)=\frac{1}{2\pi i}\int_L T_{\theta zjk}(p,\theta)r^{-p-1}dp, \quad (10)$$

$$T_{\theta zjk}(p,\theta)=-a_k[A_k(\mathrm{p})\sin p\theta+B_k(\mathrm{p})\cos p\theta]+$$
$$+(a_k\theta+b_k)p[A_k(p)\cos p\theta-B_k(p)\sin p\theta].$$

According to the regularity conditions, the integration path L is located parallel to an imaginary axis in the strip

$$-\delta_1<\operatorname{Re}p<\delta_2\ (\delta_1,\delta_2>0).$$

The quantities $A_k(p)$ and $B_k(p)$ are found from boundary conditions (7) and (8).

Following the scheme implemented in [17], we come to the inhomogeneous Wiener–Hopf equation:

$$F(p)[T_+(p)+G_-(p)]+\mu_0\varepsilon^{-1}W_-(p)=0\ (p\in L), \quad (11)$$

where

$$T_+(p)=\int_0^1\tau_{\theta z1}(\varepsilon\rho,+0)\rho^p d\rho,\ G_-(p)=\int_1^\infty g(\varepsilon\rho)\rho^p d\rho,$$

$$W_{-}(p)=\int_{1}^{\infty}\frac{\partial}{\partial\rho}[w_1(\varepsilon\rho,+0)-w_2(\varepsilon\rho,-0)]\rho^p d\rho.$$

Functions $G_{-}(p)$ and $W_{-}(p)$ are regular and do not have zeros in in the half-plane Ω_{-}left from the path L, while $T_{+}(p)$ does not have zeros in the right half-plane Ω_{+} [18]. An imaginary axis can be selected as the path L.

The coefficient of Eq. (11) takes the form

$$F(p)=\mathrm{ctg}(\alpha_1 p)\frac{v(\alpha_1 p)}{u(\alpha_1 p)}+\mathrm{ctg}(\alpha_2 p)\frac{v(\alpha_2 p)}{u(\alpha_2 p)}, \tag{12}$$

where

$$u(x)=1+m^{-1}(m-1)^2 x^{-2}[1-x\mathrm{ctg}(x)], \tag{13}$$

$$v(x)=1+(m-1)x^{-1}\mathrm{tg}(x),\ m=\sqrt{\mu_0/\mu_*}.$$

The parameter m characterizes the relative shear stiffness of the material on the crack line compared to the material on the sides of wedge. The crack is located in the region of locally soft composite material at $0 < m < 1$, and in the region of the locally rigid material at $1 < m < \infty$. The case $m = 1$ corresponds to homogeneous material in the regions Ω_k. The expression given in [17] is obtained from Eqs. (12) and (13) for the coefficient of problem (11).

To factorize function (12), let us represent it in the following form:

$$F(p)=\frac{2}{p}K(p), \tag{14}$$

$$K(p)=X(p)\Phi(p),\ X(p)=p\mathrm{ctg}(\alpha_1 p),$$

$$\Phi(p)=\frac{1}{2}F_1(p)F_2(p),\ F_1(p)=\frac{v(\alpha_1 p)}{u(\alpha_1 p)},$$

$$F_2(p)=1+\mathrm{tg}(\alpha_1 p)\mathrm{ctg}(\alpha_2 p)\frac{u(\alpha_1 p)v(\alpha_2 p)}{u(\alpha_2 p)v(\alpha_1 p)}.$$

Notice that the function $F_2(p) = 2$ at $\alpha_1 = \alpha_2$, while the function $F_1(p) = 1$ for a homogeneous medium.

Factorization of the function $X(p)$ is carried in an elementary way [18]:

$$X(p)=X_{+}(p)X_{-}^{-1}(p), \tag{15}$$

$$X_{+}(p)=\sqrt{\frac{\pi}{\alpha_1}}\frac{\Gamma(1+p\alpha_1/\pi)}{\Gamma(1/2+p\alpha_1/\pi)},\ X_{-}(p)=\sqrt{\frac{\alpha_1}{\pi}}\frac{\Gamma(1/2-\alpha_1 p/\pi)}{\Gamma(1-\alpha_1 p/\pi)}.$$

The function $\Phi(it)$ is continuous on the imaginary axis of the function at $p = it$, has no zeros and poles, its index is zero and it exponentially tends to unity at $t \to \infty$. Therefore, in accordance with the data from [18],

$$\Phi(p)=\frac{\Phi_{+}(p)}{\Phi_{-}(p)},\ \Phi_{\pm}(p)=\exp\left[-\frac{1}{2\pi i}\int_{L}\frac{\ln\Phi(t)}{t-p}dt\right]\ (p\notin L). \tag{16}$$

Because the function $\Phi(p)$ is even, analytic functions (16) in the regions Ω_{+} and Ω_{-} can be represented as

$$\Phi_{\pm}(p) = \exp\left[\frac{p}{\pi}\int_0^{\infty}\frac{\ln\Phi(i\xi)}{\xi^2+p^2}d\xi\right].$$

Using Eqs. (14)–(16), regrouping the terms in Eqs. (11) and applying Liouville's theorem [18], we obtain:

$$\Phi_+(p)X_+(p)T_+(p) + Q_+(p) = -\frac{\mu_1 p}{2\varepsilon}W_-(p)\Phi_-(p)X_-(p) - Q_-(p) = J(p), \quad (17)$$

where

$$Q_{\pm}(p) = \mp\frac{1}{2\pi i}\int_L \frac{Q(t)}{t-p}dt,\ Q(t) = \frac{t}{2}\Phi_-(t)X_-(t)F(t)G_-(t). \quad (18)$$

Estimating the terms in equality (16) with $p \to \infty$, we can conclude that the unified analytic function is $J(p) = const = C$. Let us find this constant from Eq. (17) at $p = 0$. In view of Eq. (18), we find that

$$C = C_* G_-(0) - \frac{1}{4\pi i}\int_L \Phi_-(\mathrm{t})X_-(p)F(t)G_-(t)dt, \quad (19)$$

$$C_* = \Phi_+(0)X_+(0) = \sqrt{\frac{3m^2(\alpha_1+\alpha_2)}{2\alpha_1\alpha_2(m^2+m+1)}}.$$

To calculate the integral in Eq. (19), we use Cauchy's residue theorem. The poles of the integrand in the left half-plane are the poles of $F(t)$. It follows from representation (12) that they are determined by the negative roots of the equation

$$mx^2\sin x + (m-1)^2(\sin x - x\cos x) = 0,$$

lying in the intervals

$$-(n+0.5)\pi < -x_n < -n\pi\ (n = 1,2,...).$$

There are two groups of poles: $t_{nj} = -x_n/\alpha_j$ (j = 1, 2).

We assume that concentrated forces with the magnitude T_0 are applied to the edges of the crack at a distance r_0 from the apex of the wedge. In this case,

$$g(r) = -T_0\delta(r - r_0),$$

where $\delta(r - r_0)$ is the Dirac delta function, while

$$G_-(p) = -T_0/\varepsilon(r_0/\varepsilon)^p.$$

As a result, we obtain from Eq. (19) that

$$C = \frac{T_0}{\varepsilon}\left[C_* + \frac{1}{2}\sqrt{\frac{\alpha_1}{\pi}}\sum_{j=1}^{2}\sum_{n=1}^{\infty}a_{nj}\left(\frac{\varepsilon}{r_0}\right)^{x_n/\alpha_j}\right], \quad (20)$$

where

$$a_{nj} = \frac{1}{\alpha_j} \frac{\Gamma(1/2 - \alpha_1 t_{nj}/\pi)}{\Gamma(1 - \alpha_1 t_{nj}/\pi)} \Phi_-(t_{nj}) b(x_n),$$

$$b(x_n) = \frac{x_n \cos x_n + (m-1)\sin x_n}{x_n \cos x_n + (m + m^{-1})\sin x_n}.$$

Using the procedure based on Abel-type theorem [18] (used in [17]), we conclude that the asymptotic expansion of the stresses on the crack line with $r \to \varepsilon - 0$ takes the form

$$\tau_{\theta z1}(r) \sim C\sqrt{\frac{\varepsilon}{\pi}} \frac{1}{\sqrt{\varepsilon - r}}. \tag{21}$$

We define the stress intensity factor (SIF) at the crack tip by the formula

$$K_{\mathrm{III}} = \lim_{r \to \varepsilon - 0} \sqrt{2\pi(\varepsilon - r)}\tau_{\theta z1}(r).$$

Then, using asymptote (21), we obtain:

$$K_{\mathrm{III}}(\alpha_1, \alpha_2, m, \varepsilon/r_0) = \sqrt{2\varepsilon}C. \tag{22}$$

To examine the effect from the gradient of the material, we introduce a normalized SIF of the form

$$N = K_{III}/K_{III}^0,$$

where K_{III}^0 is the SIF at the tip of the crack located in a homogeneous wedge.

According to [17], in the case of geometric symmetry, i.e., at $\alpha_1 = \alpha_2 = \alpha$, such a SIF takes the form

$$K_{\mathrm{III}}^0 = T_0\sqrt{\frac{2}{\alpha\varepsilon}} \frac{r_0^{\pi/(2\alpha)}}{\sqrt{r_0^{\pi/\alpha} - \varepsilon^{\pi/\alpha}}}. \tag{23}$$

It follows from Eqs. (20)–(23) that the crack behaves unsteadily at small distances between the crack tip and the angular point of the wedge in both a homogeneous and a gradient material, since $K_{\mathrm{III}} \to \infty$ at $\varepsilon \to 0$.

The dependence of the normalized SIF at the tip of the crack located in the composite functionally graded half-plane at $\alpha_1 = \alpha_2 = \pi/2$ on the relative distance ε/r_0 for different values of relative shear stiffness is shown in Fig. 2. If $m < 1$, the gradient of elastic properties produces a significant decrease in the magnitude of SIF compared to homogeneous material. At the same time, a decrease in the parameter m produces increasing differences in SIF values for the inhomogeneous and homogeneous cases. Conversely, the stiffening of the material along the ray $\theta = 0$ ($m > 1$) produces an increase in the SIF at the tip of the crack. These trends in the behavior of the normalized SIF occur at all other wedge opening angles (Fig. 3).

Stress singularity in the tip of the wedge

We examine the stress fields at the tip of the wedge for $r \to 0$. The tangential stresses along the ray $\theta = 0$ take the form

$$\tau_{\theta zj}(r, 0) = \frac{1}{2\pi i}\int_L [T_+(p) + G_-(p)]\left(\frac{r}{\varepsilon}\right)^{-p-1} dp. \tag{24}$$

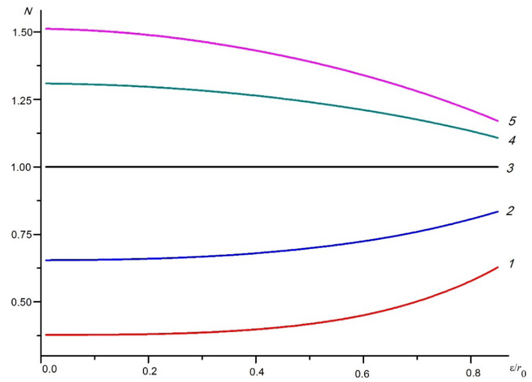

Fig. 2. Dependences of normalized SIF in the tip of the crack located in the gradient half-plane $\alpha_1 = \alpha_2 = 90°$, on the parameter ε/r_0 for different values of the relative shear stiffness *m*: 0.25 (*1*), 0.50 (*2*), 1.0 (*3*), 2.0 (*4*), 4.0 (*5*)

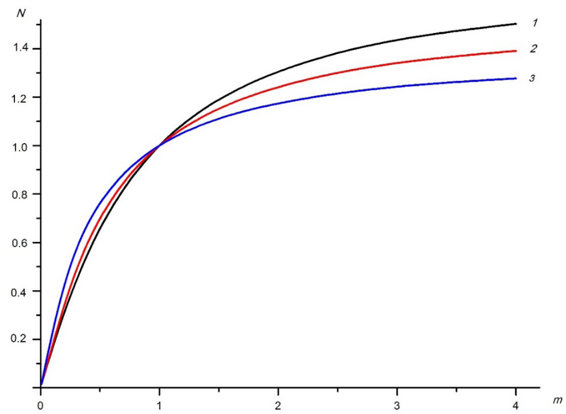

Fig. 3. Dependences of normalized SIF at the crack tip on the relative shear stiffness *m* at $\varepsilon/r_0 = 0.5$ for different values of the angle $\alpha = \alpha_1 = \alpha_2$: 30° (*1*), 90° (*2*), 180° (*3*)

Using Eq. (11) and Eqs. (14), (17) for the integrand, we obtain the following representation:

$$T_+(p) + G_-(p) = \frac{2\left[C + Q_-(p)\right]}{pK_-(p)F(p)}.$$

Based on this representation and using Eqs. (12), (13) and (24), we obtain the following expression for the stresses in the segment $0 < r < \varepsilon$ at $\theta = 0$

$$\tau_{\theta zj}(r,0) = \frac{1}{m\pi i}\int\limits_L Y(p)\frac{u_*(\alpha_1 p)u_*(\alpha_2 p)}{\Delta(p)}\left(\frac{r}{\varepsilon}\right)^{-p-1} dp, \tag{25}$$

where

$$Y(p) = \frac{C + Q_-(p)}{p^2 X_-(p)\Phi_-(p)},$$

$$u_*(x) = mx^2 \sin x + (m-1)^2(\sin x - x\cos x),$$

$$v_*(x) = x\cos x + (m-1)\sin x.$$

The poles of the integrand in Eq. (25), lying in the half-plane to the left of the path L, are determined by the roots of the equation

$$\Delta(p) = \alpha_1 u_*(\alpha_2 p) v_*(\alpha_1 p) + \alpha_2 u_*(\alpha_1 p) v_*(\alpha_2 p) = 0. \tag{26}$$

The function $\Delta(p)$ is an integer function that has a fourth-order zero at $p = 0$. However, this point is a removable singularity at $m > 0$, and the imaginary axis can be taken as the path L in equality (25). Because the function $\Delta(p)$ is even, each positive root p_k of Eq. (26) corresponds to the negative root $p_{-k} = -p_{-k}$. Since this function does not change its form if α_1 is replaced with α_2 and α_2 with α_1, it is sufficient to consider the case when $\alpha_1 \geq \alpha_2$ next.

Applying the residue theorem for the negative poles of the integrand to integral (25), we obtain the representation of stresses at $r \to 0$ in the form

$$\tau_{\theta zj}(r,0) = D_1(p_1,\alpha_1,\alpha_2,m)\left(\frac{r}{\varepsilon}\right)^{\gamma_1} + D_2(p_2,\alpha_1,\alpha_2,m)\left(\frac{r}{\varepsilon}\right)^{\gamma_2} + \ldots, \tag{27}$$

where $\gamma_k = -1 + p_k$ ($k = 1, 2, \ldots$).

It is evident that the stresses at the tip of the wedge are singular if the roots $0 < p_k < 1$ exist for the given values of the parameters α_1, α_2 and m.

In the case of a geometrically symmetric structure, where $\alpha_1 = \alpha_2 = \alpha$, it follows from Eqs. (25) and (26) that the numbers p_k are the roots of the equation

$$v_*(x) = x\cos x + (m-1)\sin x = 0 \ (x = \alpha p,\ \alpha \leq \pi). \tag{28}$$

This equation has no complex roots, and there is a single root in the interval $(0, \pi)$ for any $0 < m < \infty$, so that $0 < x_1 \leq \pi/2$ for $m \leq 1$ and $\pi/2 < x_1 < \pi$ for $m > 1$. As the relative shear stiffness parameter m decreases from unity to zero, the first root of $p_1 = x_1/\alpha$ also decreases from $\pi/(2\alpha)$ to zero. With the magnitude of m changing from unity to infinity (i.e., when the middle section of the wedge is stiffened), this root increases from $\pi/(2\alpha)$ to π/α. The dependence of the singularity exponent $\gamma = \gamma_1$ on the angle α is given in Fig. 4. Evidently, the singularity in the apex of the wedge can only be weak at $m \geq 1$ ($0 < |\gamma| < 1/2$) and occurs only for angles α greater than 90°, the same as in homogeneous material. With an increase in the parameter m, this exponent becomes smaller compared with the homogeneous case, and the range of angles at which the singularity occurs is narrowed down. In contrast to the homogeneous case, the half angles of the wedge opening at which the singularity appears become sharp, and the singularity itself can be both weak and strong ($1/2 < |\gamma| < 1$).

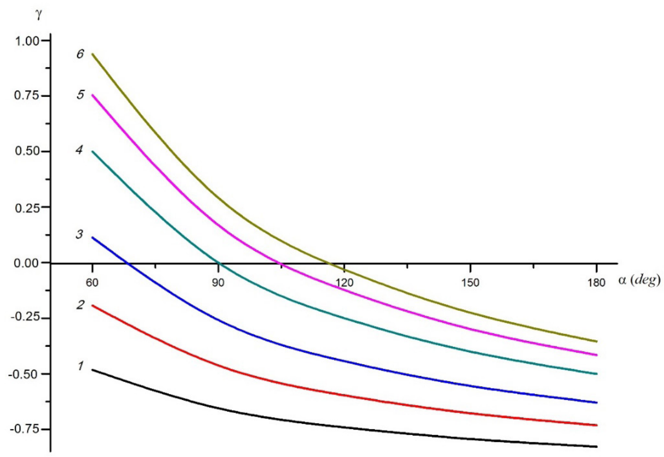

Fig. 4. Dependences of the singularity exponent γ at the tip of the functionally graded wedge on the angle $\alpha = \alpha_1 = \alpha_2$ for different values of the relative stiffness parameter m: 0.10 (*1*), 0.25 (*2*), 0.50 (*3*), 1.0 (*4*), 2.0 (*5*), 4.0 (*6*)

Analyzing the general situation when $\alpha_1 > \alpha_2$ and $\alpha_1 + \alpha_2 \le 2\pi$, let us consider a number of limiting cases.

In the case of a homogeneous wedge ($m = 1$), it follows from Eqs. (25) and (26) that the characteristic equation takes the form $\sin(\alpha_1 + \alpha_2)p = 0$, where the first root determines the classical singularity

$$\gamma_1 = -1 + \pi/(\alpha_1 + \alpha_2),$$

appearing provided that $\alpha_1 + \alpha_2 > \pi$.

Given high values of the parameter m, Eq. (26) can be written as

$$\alpha_1 f(\alpha_2 p)\sin\alpha_1 p + \alpha_1 f(\alpha_1 p)\sin\alpha_2 p = 0, \qquad (29)$$

$$f(x) = \sin x - x\cos x. \qquad (30)$$

The first positive zero x_* of function (30) lies in the interval $(\pi, 3\pi/2)$, while $f(x) > 0$ for $0 < x < x_*$ and $f(x) < 0$ for $x_* < x < 2\pi$. It follows then that Eq. (29) has no roots in the interval (0, 1) at $m >> 1$ and angles $0 < \alpha_2 < \alpha_1 \le \pi$, so there is no singularity at the corner point. Eq. (29) has a single root $1/2 < p_1 < 1$ for angles $x_* \le \alpha_1 < 2\pi$ and $0 < \alpha_2 < 2\pi - x_*$ ($x_* = 1.4302967\pi$) and large values of m, generating a weak singularity at the corner point. The presence of the root $p_1 < 1$ at $\pi < \alpha_1 < x_*$ is checked numerically.

In the case where the relative stiffness $m \to 0$, Eq. (26) takes the form

$$f(\alpha_1 p) f(\alpha_2 p) = 0, \qquad (31)$$

and the function $u_*(\alpha_1 p)u_*(\alpha_2 p)/\Delta(p)$ included in integral (25) tends to unity. However, in reality, the low values of the parameter $m = \sqrt{\mu_0/\mu_*}$ must exceed a certain value $m_* > 0$. At the same time, the limit equation (31) indicates that the first root is located near zero at sufficiently small m. Additionally, another second root of Eq. (26), which is less than unity, exists in the case of sharp notches where the angles satisfy the conditions $x_* \le \alpha_1 < 2\pi$, $0 < \alpha_2 < 2\pi - x_*$. For example, there are two roots at $\alpha_1 = 3\pi/2$, $\alpha_2 = \pi/6$ and $m = 0.10$: $p_1 = 0.3379652$ and $p_2 = 0.9599646$. Asymptote (27) contains two singular terms. Notably, the singularity generated by the second root is very weak. Numerical analysis indicates that this property is also preserved for other values of the structure parameters.

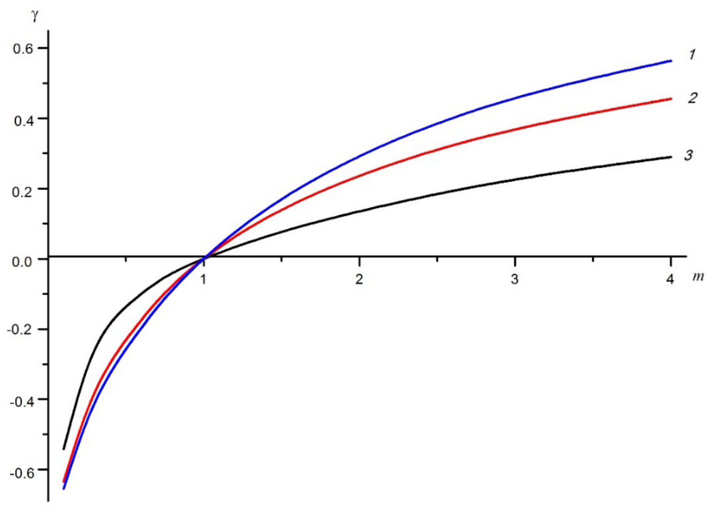

Fig. 5. Dependences of singularity exponent γ at the point $r = 0$ of the functionally graded half-plane on the relative shear stiffness m for different angles: $\alpha_1 = \alpha_2 = 90°$ (*1*); $\alpha_1 = 120°$, $\alpha_2 = 60°$ (*2*); $\alpha_1 = 150°$, $\alpha_2 = 30°$ (*3*)

Next, let us consider two particular cases in more detail. The first one is the case of a functionally graded half-plane with a semi-infinite notch when $\alpha_1 + \alpha_2 = \pi$ ($\alpha_1 \geq \alpha_2$). The analysis indicates that no stress singularity can be detected at $m \geq 1$, while the asymptotic expansion of stresses at the point $r = 0$ has one singular term at $m < 1$. Fig. 5 shows the dependence of the quantity $\gamma_1 = \gamma$ on the relative shear stiffness for different angles α_1 and α_2. Evidently, the inhomogeneity of the material at $m < 1$ produces singular stresses at the smooth half-plane boundary at the point $r = 0$. At the same time, the singularity can be both weak and strong (for fairly low m). The asymmetric position of the crack weakens the singularity to some extent.

In the case of a functionally graded plane with two notched cracks ($\alpha_1 + \alpha_2 = 2\pi$, $\alpha_1 \geq \alpha_2$), Eq. (26) can have one or two roots in the interval (0, 1). For example, if the cracks are collinear ($\alpha_1 + \alpha_2 = \pi$), there is only one root in this interval generating a strong stress singularity at the tip of the unloaded fracture at $m < 1$ and a weak singularity at $m > 1$. In the case of orthogonal cracks, when $\alpha_1 = 3\pi/2$, $\alpha_2 = \pi/2$, the characteristic equation has only one root $1/2 < p_1 < 1$ at $m > 1$, and two roots at $m < 1$: $0 < p_1 < 1/2 < p_2 < 1$. Here the second root is very close to unity and determines a weak singularity.

Conclusion

We used the Wiener–Hopf method to obtain an accurate solution to the problem on the equilibrium of a functionally graded composite wedge weakened by a semi-infinite longitudinal-shear interface crack whose edges are loaded with self-balanced forces. It was assumed that the gradient properties of materials quadratically depend on the angular coordinate. We have considered the effect of the structural parameter on the SIF in the tip of the crack. It is established that the crack becomes unstable as the distance from the crack tip to the wedge corner point tends to zero. The gradient properties of materials can considerably affect the magnitude of SIF. If the middle section of the wedge where the crack is located is relatively softer than the regions near its edges, the SIF decreases substantially compared to its value in the homogeneous material. Conversely, the stiffening of this region tends to increase the SIF compared to the homogeneous case.

The problem of stress singularity at the tip of the functionally graded wedge has a number of peculiarities compared to the case of a homogeneous structure. Unlike homogeneous material, no stress singularity appears at the tip with sufficiently high values of relative shear stiffness, even in the cases of sharp notches. On the other hand, the stresses at the tip can grow indefinitely in functionally graded wedges with sharp opening angles and a soft middle section. Moreover, the relative stiffnesses less than unity correspond to such opening angles of the wedge-shaped region at which the asymptotic expansion of stresses near its tip has two singular terms.

REFERENCES

1. **Jin Z.-H., Batra R. C.**, Some basic fracture mechanics concepts in functionally graded materials, J. Mech. Phys. Sol. 44 (8) (1996) 1221–1235.

2. **Abotula A., Kidane A., Chalivendra V. B., Shukla A.,** Dynamic curving cracks in functionally graded materials under thermomechanical loading, Int. J. Solids Struct. 49 (4) (2012) 583–593.

3. **Mostefa A. H., Merdai S., Mahmoudi N.**, An overview of functionally graded materials 'FGM', In book: Proceedings of the Third International Symposium on Materials and Sustainable Development, Ed. by Abdelbaki B., Safi B., Saidi M. Springer Cham (2018) 267–278.

4. **Carpinteri A., Paggi M.,** Asymptotic analysis in linear elasticity: from the pioneering studies by Westerhardt and Irwin until today, Eng. Fract. Mech. 76 (12) (2009) 1771–1784.

5. **Carpinteri A., Paggi M.,** On the asymptotic stress field in angularly nonhomogeneous materials, Int. J. Fract. 135 (1–4) (2005) 267–283.

6. **Cheng C. Z., Ge S. Y., Yao S. I., et al.,** Singularity analysis for a V-notch with angularly inhomogeneous elastic properties, Int. J. Solids Struct. 78–79 (1) (2016) 138–148.

7. **Erdogan F.,** Crack problems for bonded nonhomogeneous materials under antiplane shear loading, J. Appl. Mech. 52 (4) (1985) 823–828.

8. **Erdogan F., Ozturk M.,** Periodic cracking of functionally graded coatings, Int. J. Eng. Sci. 33 (15) (1995) 2179–2195.

9. **Jin Z.-H., Batra R. C.,** Interface cracking between functionally graded coatings and a substrate under antiplane shear, Int. J. Eng. Sci. 34 (15) (1996) 1705–1716.

10. **Li Y.-D., Lee K. Y.,** An antiplane crack perpendicular to the weak/microdiscontinuos interface in a bi-FGM structure with exponential and linear nonhomogeneities, Int. J. Fract. 146 (4) (2007) 203–211.

11. **Pan H., Song T., Wang Z.,** An analytical model for collinear cracks in functionally graded materials with general mechanical properties, Compos. Struct. 132 (15) (2015) 359–371.

12. **Linkov A., Rybarska-Rusinek L.,** Evaluation of stress concentration in multi-wedge systems with functionally graded wedges, Int. J. Eng. Sci. 61 (1) (2012) 87–93.

13. **Tikhomirov V. V.,** Stress singularity in a top of the composite wedge with internal functionally graded material, St. Petersburg State Polytechnical University Journal. Physics and Mathematics. (3 (225)) (2015) 96–106.

14. **Makhorkin M. I., Skrypochka T. A., Torskyy A. R.,** The stress singularity in a composite wedge of functionally graded materials under antiplane deformation, Math. Model. Comput. 2020. Vol. 7 (1) (2020) 39–47.

15. **Wang Y.-S., Huang G.-Y., Dross D.,** On the mechanical modeling of functionally graded interfacial zone with Griffith crack: antiplane deformation, J. Appl. Mech. 70 (5) (2003) 676–680.

16. **Guo L.-C., Noda N.,** Modeling method for a crack problem of functionally graded materials with arbitrary properties – piecewise-exponential model, Int. J. Solids Struct. 44 (15) (2007) 6768–6790.

17. **Tikhomirov V. V.,** A semi-infinite crack of mode III in the bimaterial wedge, St. Petersburg State Polytechnical University Journal. Physics and Mathematics. (2(242)) (2016) 126–135.

18. **Noble B.**, Method based on the Wiener – Hopf technique for solution of partial differential equations, Pergamon Press, New York, London, 1958.

СПИСОК ЛИТЕРАТУРЫ

1. **Jin Z.-H., Batra R.C.** Some basic fracture mechanics concepts in functionally graded materials // Journal of Mechanics and Physics of Solids. 1996. Vol. 44. No. 8. Pp. 1221–1235.

2. **Abotula A., Kidane A., Chalivendra V. B., Shukla A.** Dynamic curving cracks in functionally graded materials under thermomechanical loading // International Journal of Solids and Structures. 2012. Vol. 49. No. 4. Pp. 583–593.

3. **Mostefa A. H., Merdai S., Mahmoudi N.** An overview of functionally graded materials ‘FGM’ // Proceedings of the Third International Symposium on Materials and Sustainable Development. Edited by Abdelbaki B., Safi B., Saidi M. Springer Cham, 2018. Pp. 267–278.

4. **Carpinteri A., Paggi M.** Asymptotic analysis in linear elasticity: from the pioneering studies by Westerhardt and Irwin until today // Engineering Fracture Mechanics. 2009. Vol. 76. No. 12. Pp. 1771–1784.

5. **Carpinteri A., Paggi M.** On the asymptotic stress field in angularly nonhomogeneous materials. // International Journal of Fracture. 2005. Vol. 135. No. 1–4. Pp. 267–283.

6. **Cheng C. Z., Ge S. Y., Yao S. I., Niu Z. R., Recho N.** Singularity analysis for a V-notch with angularly inhomogeneous elastic properties // International Journal of Solids and Structures. 2016. Vol. 78–79. No. 1. Pp. 138–148.

7. **Erdogan F.** Crack problems for bonded nonhomogeneous materials under antiplane shear loading // Journal of Applied Mechanics. 1985. Vol. 52. No. 4. Pp. 823–828.

8. **Erdogan F., Ozturk M.** Periodic cracking of functionally graded coatings // International Journal of Engineering Science. 1995. Vol. 33. No. 15. Pp. 2179–2195.

9. **Jin Z.-H., Batra R. C.** Interface cracking between functionally graded coatings and a substrate under antiplane shear // International Journal of Engineering Science. 1996. Vol. 34. No. 15. Pp. 1705–1716.

10. **Li Y.-D., Lee K. Y.** An antiplane crack perpendicular to the weak/microdiscontinuos interface in a bi-FGM structure with exponential and linear nonhomogeneities // International Journal of Fracture. 2007. Vol. 146. No. 4. Pp. 203–211.

11. **Pan H., Song T., Wang Z.** An analytical model for collinear cracks in functionally graded materials with general mechanical properties // Composite Structures. 2015. Vol. 132. No. 15. Pp. 359–371.

12. **Linkov A., Rybarska-Rusinek L.** Evaluation of stress concentration in multiwedge systems with functionally graded wedges // International Journal of Engineering Science. 2012. Vol. 61. No 1. Pp. 87–93.

13. **Тихомиров В. В.** Сингулярность напряжений в вершине композитного клина с внутренним функционально-градиентным материалом // Научно-технические ведомости СПбГПУ. Физико-математические науки. 2015. № 3 (225). С. 96–106.
14. **Makhorkin M. I., Skrypochka T. A., Torskyy A. R.** The stress singularity order in a composite wedge of functionally graded materials under antiplane deformation // Mathematical Modelling and Computing. 2020. Vol. 7. No. 1. Pp. 39–47.
15. **Wang Y.-S., Huang G.-Y., Dross D.** On the mechanical modeling of functionally graded interfacial zone with Griffith crack: antiplane deformation // Journal of Applied Mechanics. 2003. Vol. 70. No. 5. Pp. 676–680.
16. **Guo L.-C., Noda N.** Modeling method for a crack problem of functionally graded materials with arbitrary properties – piecewise-exponential model // International Journal of Solids and Structures. 2007. Vol. 44. No. 15. Pp. 6768–6790.
17. **Тихомиров В. В.** Полубесконечная трещина моды III в биматериальном клине // Научно-технические ведомости СПбГПУ. Физико-математические науки. 2016. № 2 (242). С. 126–135.
18. **Noble B.** Method based on the Wiener – Hopf technique for solution of partial differential equations. New York, London: Pergamon Press, 1958. 246 p.

THE AUTHOR

TIKHOMIROV Victor V.
Peter the Great St. Petersburg Polytechnic University
29 Politechnicheskaya St., St. Petersburg, 195251, Russia
victikh@mail.ru
ORCID: 0000-0001-9655-5817

СВЕДЕНИЯ ОБ АВТОРЕ

ТИХОМИРОВ Виктор Васильевич – *кандидат физико-математических наук, заместитель директора по образовательной деятельности Института прикладной математики и механики Санкт-Петербургского политехнического университета Петра Великого.*
195251, Россия, г. Санкт-Петербург, Политехническая ул., 29
victikh@mail.ru
ORCID: 0000-0001-9655-5817

Received 29.04.2022. Approved after reviewing 30.08.2022. Accepted 30.08.2022.
Статья поступила в редакцию 29.04.2022. Одобрена после рецензирования 30.08.2022. Принята 30.08.2022.